Se-Methylselenocyteine, D-α-Tocopheryl Succinate, β-Carotene and L-Lysine Combined Can Prevent Cancer Metastases as an Adjuvant Therapy

Shuhui Li
Fuzhou University - Yishan Campus: Fuzhou University
Yunlong Cheng
Fuzhou University - Yishan Campus: Fuzhou University
Shu Lian
MJU: Minjiang University
Yusheng Lu
Minjiang University
Jie Wang
Fuzhou University - Yishan Campus: Fuzhou University
Xiaoxiao Deng
Fuzhou University - Yishan Campus: Fuzhou University
Shengyi Zhai
Fuzhou University - Yishan Campus: Fuzhou University
Lee Jia (cmapcjia1234@163.com)
Fuzhou University https://orcid.org/0000-0001-6839-5545

Research Article

Keywords: Cancer prevention, Cancer metastases, Se, Combination drugs

Posted Date: July 7th, 2021

DOI: https://doi.org/10.21203/rs.3.rs-660120/v1

Abstract

Primary tumour treatment by surgical resection and adjuvant therapy has been extensively studied, but there is a lack of effective strategies and drugs for the treatment of tumour metastases. Here, we show a functional combined product based on their individual well-known mechanisms for inhibiting cancer metastases, improving anti-cancer treatment, and enhancing immunity and antioxidant capacity as an adjuvant therapy. MVBL, our designed combination, consists of four inexpensive compounds: L-Se-methylselenocysteine, D-α-tocopheryl succinate, β-carotene and L-lysine. In this study, MVBL exhibited higher toxicity toward tumour cells than toward normal cells. It did not significantly affect the cancer cell cycle but increased their apoptosis. Wound healing, adhesion, and transwell assays showed that MVBL significantly inhibited tumour cell migration, adhesion and invasion. MVBL sensitized MDA-MB-231 breast cancer cells to paclitaxel, indicating that MVBL had a synergistic effect as an adjuvant. In addition, animal experimental data showed that MVBL inhibited mouse tumour cell metastasis, prolonged survival time, and enhanced antioxidant capacity and immune function in mice. In summary, this study reveals the roles of MVBL in improving immunity and antioxidation, preventing tumour growth, and inhibiting metastasis in vitro and in vivo. MVBL may be used as an adjuvant cancer therapy for improving survival and quality of life among cancer patients.

1. Introduction

Cancer remains the second leading cause of death worldwide(1). Although surgical resection and adjuvant therapy can be used to treat primary tumours, most tumour patients have risks of tumour recurrence and metastasis after surgery; indeed, postoperative metastasis is the main cause of death among cancer patients. Reactive oxygen species (ROS) are oxygen-containing active chemicals produced by chemical reactions in living organisms, and a variety of studies have found that ROS are involved in malignant transformation of cells(2). Excessive ROS can induce such malignant transformation by regulating transcription factors (c-MYC/p53/HIF-1α)(3), promote tumour cell invasion by targeting kinases and transcription factors, and influence other tumour-associated signalling pathways. Studies have shown that tumour cells with higher ROS levels have higher migration and invasion capacities(4). However, antioxidant treatment has been found to reduce ROS levels in xenograft nude mouse models in vivo and to inhibit hypoxia-induced metastasis in human pancreatic cancer cells(5, 6). In non-small cell lung cancer, ROS lead to tumour metastasis by modulating lipopolysaccharide-mediated TLR4 signalling. High levels of ROS in mitochondria promote cell proliferation, survival, migration, and epithelial-mesenchymal transition by activating extracellular signals to regulate mitogen-activated protein kinase and Ras-ERK(7).

Prevention of tumour metastasis is key to the effective treatment of tumours. After surgery, chemotherapy, and radiotherapy, patients with low immune function and metabolic disorders need exogenous nutrient supplementation in order to improve their metabolic states and antitumour treatment tolerance and in order to reduce complications and adverse reactions. Based on this information, we comprehensively analysed the mechanisms of tumour production, development and metastasis and the

characteristics of circulating tumour cells (CTCs) in the blood and then formulated a corresponding preventive and adjuvant treatment, namely, MVBL, which contains four components: L-selenium-methylselenocysteine (MSC), D-α-tocopherol succinic acid (VES), beta-carotene (β-Ca) and lysine (Lys) (see Fig. S1 for the structural formulae). As early as 2003, the FDA confirmed that selenium is a cancer suppressant. Selenium has an antioxidant effect that inhibits the production of free radicals and reduces the risk of cancer caused by peroxidation(8–10). Selenium also enhances human immune function by promoting lymphocyte proliferation(11–14) and tumour cell apoptosis(15–17). VES, a derivative of vitamin E esterification, is one of the most potent antitumour compounds in the vitamin E family. β-Ca prevents tumour formation by regulating the levels of cytochrome P450 and glutathione transferase (GST) in vivo(18). It also inhibits the metastasis and invasion of neuroblastoma by decreasing the levels of HIF-α(19). L-Lys is an essential amino acid in the human body. It not only participates in the synthesis of proteins(20) but also binds to the active site of fibrinogen to reduce fibrinogen production, thus protecting the matrix, promoting the production of collagen, strengthening the structure of the tissue matrix, reducing the enveloping of connective tissue around tumour cells, and effectively inhibiting the secretion of matrix metalloproteinases (MMPs)(21, 22). Thus, a combination of the above four substances will not only serve as a nutrient supplement but also effectively prevent the metastasis of postoperative tumours.

Here, we prepared MVBL, performed antitumour metastasis studies in vitro and investigated the effects of MVBL on tumour migration and invasion and tumour cell adhesion. When used in combination with paclitaxel (PTX), MVBL enhanced the therapeutic effects of PTX and the antioxidation effects of PTX in vitro. We also performed in vivo experiments to analyse the effects of MVBL with regard to antioxidation, immune enhancement, metastasis inhibition and life expectancy. The results indicated that MVBL may significantly improve physiological nutritional status and organ function and enhance nutritional metabolism in patients undergoing surgery, chemotherapy and radiation therapy. It may aid in cancer treatment, ameliorate energy and nutrient abnormalities, promote healing, reduce complications and adverse reactions, and effectively improve patient tolerance to cancer treatment. MVBL may also inhibit tumour metastasis and improve immunity.

2. Methods

2.1 MVBL composition

MVBL consists of the following substances: L-Se-methylselenocysteine (Jiangxi Chuanqi Pharmaceutical Co., Ltd., China), D-α-tocopheryl succinate (Sigma, America), β-carotene (Sigma, America) and L-lysine (Aladin, shanghai), Drug doses were chosen based on the human doses of the four drugs and converted to mouse doses according to the body surface area index.

2.2 Cell culture

Human breast cancer cells MDA-MB-231 and MCF-7, human cell lung cancer cells A549, mouse breast cancer cells 4T1, human colon cancer cells HT29, human normal liver cells LO2, human lung fiber cells

HELF were purchased from the Type Culture collection of the Chinese Academy of Science (Shanghai, China). All cells cultured in medium containing 10% FBS and 1% penicillin/streptomycin in a humidified atmosphere with 5 % CO_2 at 37 ℃.

2.3 Cell viability assay

The cytostatic effects were determined by using the 3-(4, 5- dimethylthiazol-2-yl)-2, 5-diphenyltetrazolium bromide (MTT) assay. Cells were seeded into the 96-well plates at 10×10^4/cell, after incubating at 37°C for 24 h, the supernatant was replaced with the medium containing different concentrations of single drugs and MVBL (no.1–9, Fig. 1f), and 5 replicate wells were set for each sample. After 24 h, the medium was aspirated, and MTT solution was added for 4 h, finally formazan dissolved in DMSO and the absorbance was measured under a microplate reader (490 nm/570 nm). Cell viability was calculated from the absorbance.

2.4 Cell cycle and apoptosis assays

The cell cycle was detected by staining the nucleus with PI. A549, MCF-7, MDA-MB-231 cells were seeded in 6-well plates and incubated with single drugs and different concentrations of MVBL (Table S1). After 24 h, the cells were digested and centrifuged, and washed twice with pre-cooled PBS and fixed in 70% ice-cold ethanol overnight. After centrifuging the ethanol, 500 μL of prepared PI was added to each tube, and dyed it in the dark at 37℃ for 40 min. The cell cycle distribution was determined by flow cytometry (BD Biosciences) with laser excitation set at 488 nm.

Consistent with the cell cycle dosing method described above, the supernatant medium was collected after incubation with the drugs for 24 hours, and centrifuged with the digested cells. After washing twice with pre-cooled PBS, 500 μL of Binding buffer and 5 μL of Annexin-V FITC and 10 μL of PI were added to each tube. The cells were incubated for 15 minutes at room temperature in the dark, and detected by flow cytometry.

2.5 Cell migration and cell invasion assays

The cells were seeded in a 12-well plates. After the monolayer cells completely covered the bottom, three lines were drawn vertically in each well and washed with PBS (2%), then different concentrations of MVBL (Table S2, Low/High) were added. The scratch width of each well was observed under the fluorescence microscope at 0 h and 24 h, respectively, and the migration distances in MVBL and the control group were calculated and compared.

The invasive ability of the cells was examined by transwell experiment. Matrigel was first placed at the bottom of the chamber, then the MVBL-containing medium was prepared by incomplete medium containing 0.1% BSA and suspended the cells. 250 μL of a cell suspension containing MVBL was added to each chamber. Outside of the chamber, 750 μL of 20% FBS-containing medium was added, and the culture was continued for 24 h. Five fields were randomly selected under the microscope to take a picture and counted the number of cells penetrating the chamber, and compared the numbers.

2.6 Analysis of the effects of combined MVBL and PTX treatment

MTT experiments, cell cycle and apoptosis experiments were used to detect the effects of MVBL combined with PTX. We determined the inhibition of PTX on breast cancer cells (MDA-MB-231) by MTT assay, and selected concentration above the IC50 value (6.25 μM) to combine with various concentrations of MVBL (Fig. 4E). Based on the MTT results, we further examined their effects on cell cycle and apoptosis: (1) control, (2) PTX (6.25 μM) + MVBL (no.1), (3) PTX (6.25 μM) + MVBL (no.4), (4) PTX (6.25 μM), (5) PTX (12.5 μM). The methods have been described above.

2.7 Effects of MVBL on ROS in tumour cells

Different concentrations of the single drugs and MVBL (Table S2) were incubated with MCF-7 cells in a 6-well plate for 24 h, 10×10^4 cells were collected in a centrifuge tube and washed 3 times with PBS. The prepared DCFH-DA was added and incubated at 37℃ for 20 min. After the staining was completed, it was washed 3 times with PBS, and a flow cytometer was used for laser detection at a wavelength of 488 nm.

2.8 In vivo analyses of antioxidant capacity and immunity

Kunming mice (females, age, 6-8weeks) were purchased from Shanghai SLAC Laboratory Animal Co., Ltd. (Shanghai, China). They were randomly divided into 4 groups (n = 10), including the control and MVBL (Low, Medium, High) groups (Table S3). VES and β-Ca were dissolved in oil, MSC and Lys were dissolved in water, than mixed the two solution to form an oil-water mixture, and the mice were orally inoculated with 200 μL for 30 consecutive days. The mice were weighed the day before the gavage and weighed once every three days until the 30th day of gavage.

2.9 Immunity assay

Flow cytometry was used to detect changes in T cells in mice. Blood was taken from the eyelids on days 0 and 15 after intragastric administration, and the anticoagulant EDTA was added. Then, 1.25 μL of CD8a-perCP antibody and 2.5 μL of CD3e-PE antibody were added, and the samples were incubated for 20 minutes. After that, ACK lysis buffer was added, and the samples were incubated for 3 minutes before being centrifuged at 400 × *g* for 5 minutes; this step was repeated twice. Then, 400 μL of PBS containing 1% FBS was added, and the samples were analysed by flow cytometry (488 nm). The proportions of T cells were recorded.

Two hours after the last gavage, the mice were injected with India ink (0.01 mL/g) in the tail vein. At the 2nd and 8th minute, 10 μL of blood was taken from the orbit, and 1 mL of Na_2CO_3 (0.1%) was added. The absorbance was then measured under a microplate reader at 580 nm. The carbon clearance (K) was calculated ($K = (\log A_1-\log A_2)/(t_2-t_1)$)*. After the blood was collected, the mice were weighed and sacrificed. The spleen was dissected from each mouse and weighed to calculate the spleen index (spleen index=(spleen weight/mouse weight) ×10).

*t_1 is the second minute, and t_2 is the eighth minute. A_1 is the absorbance of the blood sample taken at 2 minutes, and A_2 is the absorbance of the blood sample taken at 18 minutes.

2.10 Antioxidant capacity assay

Blood was taken from the eyelids on the 15th day and the 30th day after intragastric administration, and 4% sodium citrate was added for anticoagulation. The samples were then centrifuged at 600 × *g* for 10 minutes at 4°C. The serum supernatant was collected and stored at -80°C.

First, the total antioxidant capacity (T-AOC) of the mice was measured. $FeSO_4 \cdot 7H_2O$ standard solutions (1.5, 1.2, 0.9, 0.6, and 0.3 mM) and 2,4,6-tripyridyl-S-triazine (TPTZ)-containing ferric reducing antioxidant power (FRAP) working solutions were prepared; 5 μL of $FeSO_4$ was added to 180 μL of each FRAP working solution to make a standard solution. For each sample, five microlitres of serum was added to 180 μL of FRAP working solution, and 5 μL of ultrapure water was added for the control group. The solutions were placed in 96-well plates and tested at 593 nm. The T-AOC in the blood was determined by calculating the TPTZ content.

Second, the malondialdehyde (MDA) content in the blood of mice was measured. Briefly, 200 μL of MDA detection working solution and 50 μL of serum (control/low/medium/high), 50 μL of PBS for the blank control, or 50 μL of standard solution (1/2/5/10/20/50 μM) were added to a 200 μL centrifuge tube. The samples were incubated at 100℃ for 15 minutes and then centrifuged (100 × *g*, 5 minutes), and the supernatant was removed and added to a 96-well plate for detection with a microplate reader (450 nm). The MDA content was calculated according to the standard curve.

Finally, superoxide dismutase (SOD) activity in blood was measured. A total of 151 μL of SOD detection buffer, 8 μL of WST-8, and 1 μL of enzyme solution were mixed to make a WST-8 working solution. There were 6 samples: the (1) control 1 (SOD detection buffer 20 μL + WST-8 working solution 160 μL + initiation solution 40 μL), (2) control 2 (WST-8 working solution 160 μL + initiation solution 40 μL), (3) control 3 (control serum 20 μL + WST-8 working solution 160 μL + initiation solution 20 μL), (4) low (low serum 20 μL + WST-8 working solution 160 μL + initiation solution 20 μL), (5) medium (medium serum 20 μL + WST-8 working solution 160 μL + initiation solution 20 μL), and (6) high (high serum 20 μL + WST-8 working solution 160 μL + initiation solution 20 μL) samples. The absorbance was measured at 450 nm with a microplate reader.

% Inhibition = $[(A_{control\ 1}-A_{control\ 2})-(A_{sample}-A_{control\ 3})]/(A_{control\ 1}-A_{control\ 2}) \times 100\%$; SOD enzyme activity=% inhibition/(1-%inhibition)

2.11 In vivo metastasis analysis

BALB/c mice (females; age, 6-8weeks) were purchased from Shanghai SLAC Laboratory Animal Co., Ltd. (Shanghai, China). They were randomly divided into 4 groups (n = 6), which received an intravenous injection of PBS (200 μL, PH = 7.4) containing 4T1 cells (5.0×10^4) into the tail vein. The mice were

sacrificed 15 days after gavage of the same dose as above, and the lungs of the mice were dissected and placed in Bouin's solution 24 hours for pulmonary nodule counting.

3. Results

3.1 MVBL inhibited tumour cell activity more strongly than single drugs

We detected the inhibitory effects of MVBL in several tumour cell lines, including the A549, MDA-MB-231, HT-29, MCF-7 and 4T1 cell lines. We first examined the inhibitory effect of each ingredient on the different tumour cells to determine the concentration to use for MVBL. The MTT assay results showed differences in the sensitivities of the different cells to the different drugs. β-Ca at high concentrations was most toxic to A549 and MDA-MB-231 cells (Fig. 1A), Lys had almost no toxicity (Fig. 1B), MSC was most toxic to A549 and MDA-MB-231 cells (Fig. 1C), and VES was most toxic to HT-29 and MDA-MB-231 cells (Fig. 1D). We also tested the effects on normal cells, such as LO2 and HELF cells, and the drugs showed lower toxicity to normal cells than to tumour cells. MVBL had obvious inhibitory effects on various tumour cell types (Fig. 1E) at different concentrations (Fig. 1F). The MTT experiments showed that MVBL was more lethal to tumour cells than the single drugs. We chose concentrations above the half-maximal inhibitory concentration (IC50) for the next assays. We hoped to alter the behaviour of CTCs by inhibiting cell proliferation, such as by inhibiting tumour metastasis without killing tumour cells, and to minimize side effects.

3.2 MVBL had little effect on the cell cycle and slightly promoted apoptosis

The cell cycle and apoptosis are important aspects of cell growth and proliferation, so we examined the effects of different concentrations of MVBL on the cell cycle and apoptosis in tumour cells (Table S1). We chose A549 cells for testing. The results showed that MVBL induced no obvious cell cycle arrest (Fig. 2A), but the proportion of cells in early apoptosis increased with increasing MVBL concentration (Fig. 2B). However, at the selected concentration, MVBL did not cause apoptosis in a large number of cells.

3.3 Inhibition of migration and invasion by MVBL

Migration and invasion are important processes in tumour metastasis. If drugs can inhibit these processes, they can inhibit metastasis. Due to the occurrence of contact inhibition in tumour cells, we used scratch assays to verify the ability of MVBL to inhibit migration. Compared with the control, MVBL significantly inhibited the migration of A549, MCF-7 and MDA-MB-231 cells (Fig. 3A), decreasing mobility by 18%, 12% and 15% at low concentrations and 38%, 24%, and 29% at high concentrations, respectively. We used transwell chambers to verify the inhibition of tumour cell invasion by MVBL. As shown in

Fig. 3B, the numbers of cells penetrating the chambers decreased significantly upon treatment with different MVBL concentrations. Combined with the results of the cytotoxicity assays, these results indicated that MVBL could inhibit tumour cell migration, adhesion and invasion at the selected concentration but did not kill cells.

3.4 MVBL promoted the sensitivity of tumour cells to PTX

PTX, a first-line treatment for breast cancer, has greater side effects and induces greater drug resistance when used at high doses. The MTT assay results showed that low concentrations of PTX did not have strong lethal effects on MDA-MB-231 cells (Fig. 4A); the cell survival rates were 70% (3.12 μM PTX) and 55% (6.25 μM PTX). However, when PTX was used at 25 μM, the cell viability was only 27%. We finally chose 6.25 μM PTX to use in combination with MVBL. This dose had a certain inhibitory effect on tumour cells but fewer side effects than the higher doses. The results indicated that when PTX was used in combination with MVBL, it was most toxic to MDA-MB-231 cells (Fig. 4C). We further examined the effects of treatment on cell proliferation by flow cytometry. The results revealed that MVBL combined with PTX (6.25 μM) exerted the same effect as 12.5 μM PTX alone, and more cells were retained in the S phase and the G2/M phase after combined treatment than after single-drug treatment (Fig. 4F). In addition, more apoptosis occurred in the group treated with MVBL combined with 6.25 μM PTX than in the group treated with 12.5 μM PTX alone (Fig. 4G). These results indicated that MVBL could enhance the killing effect of PTX on tumour cells, specifically by reducing cell survival, promoting apoptosis and inhibiting cell proliferation.

3.5 MVBL reduced ROS levels

In addition to Lys, the remaining three ingredients in MVBL had strong antioxidant capacity. 2',7'-Dichlorodihydrofluorescein diacetate (DCFH-DA) is a nonlabelled oxidation-sensitive probe that can be hydrolysed by intracellular esterase to form DCFH, which cannot pass through the cell membrane. DCFH can be oxidized by intracellular ROS to form DCF, which is fluorescent. Therefore, the intensity of DCF fluorescence can be measured by flow cytometry to determine intracellular ROS content. ROS levels in MCF-7 cells decreased with increasing MVBL concentration (Fig. 5A). Excessive ROS is beneficial to the malignant metastasis of tumours. MVBL could reduce the levels of free oxygen species in cells and further reduce the probability of tumour metastasis.

3.6 MVBL enhanced antioxidant capacity in vivo

Due to metabolic abnormalities, the levels of ROS are higher in tumour tissues than in normal tissues, which plays an important role in the occurrence and development of tumours. Here, we collected blood from the eyelids of mice on the 15th and 30th days after gavage to detect the relationships between treatment duration/dose and T-AOC, SOD, and MDA levels. Figure 5B shows that after 15 days of gavage, the T-AOC levels of the low-, medium- and high-dose groups were 1.44, 1.66 and 1.98 times that of the control group; after 30 days, they were 1.47, 3.04 and 3.83 times that of the control group. In addition, the

T-AOC in mouse plasma was enhanced with increasing dose and prolonged administration time. SOD levels in mouse plasma also increased with time and dose. Analyses of these two indicators showed that the antioxidant capacity of mice became stronger with treatment. MDA is another indicator of oxidative capacity; specifically, it is an indicator of lipid membrane peroxidation in mice. Contrary to the situations for T-AOC and SOD, a higher MDA content indicates a higher degree of oxidation. Figure 5B shows that MDA decreased with time and dose. The above data showed that MVBL had a strong antioxidation capacity; thus, it could remove ROS in vivo, maintain homeostasis, prevent tumours and inhibit metastasis.

3.7 MVBL enhanced immunity in vivo

We tested immunity in mice in two ways. First, we tested the changes in carbon particle clearance and spleen weight in the control and experimental groups; second, we measured the changes in the proportion of T cells in the blood. After carbon particles were injected into the tail vein, the blood flowed to the liver and spleen, where the particles were phagocytosed and eliminated by macrophages. As shown in Fig. 5C, the carbon particle clearance index increased with dose. Spleen weight was also increased in the drug-administered groups; it was heaviest in the medium-dose group, probably due to the absorption burden in the mice in the high-dose group (Fig. 5D). The proportion of T lymphocytes in the medium-dose group was also improved compared with that in the untreated group (Fig. 5E). The results of the above three experiments suggested that MVBL had the ability to enhance the immune function of mice so that the mice could resist disease with their own immune systems.

3.8 MVBL treatment suppressed cancer metastasis in vivo

MVBL had a significant inhibitory effect on tumour metastasis in vivo. We formed a lung metastasis model by injecting 4T1 cells into the tail veins of mice and then counted the tumour nodes in the lungs. As shown in Fig. 6C, the average number of lung nodules in the control group was 76, while those in the the low-, medium-, and high-dose groups were 73, 49, and 45, respectively. The average number of lung nodules decreased with increasing dose. As shown by the survival curve (Fig. 6A), MVBL significantly prolonged the survival times of mice. Compared with the control group, the three experimental groups exhibited ameliorative effects, and the medium-dose treatment was the most effective. During the experiment, there were no obvious differences in mouse body weight changes (Fig. 6B).

4. Discussion

In this article, we propose a new combination of drugs to inhibit cancer metastasis that will not only increase patients' antioxidant capacity but also supplement their nutrition. We demonstrated that MVBL had excellent inhibitory effects on a variety of tumour cell types, including A549, MDA-MB-231, HT29, and MCF-7 cells (Fig. 1). The inhibition of migration, adhesion and invasion indicated that MVBL could reduce the metastatic capacity of tumour cells (Fig. 3), and it is also expected to inhibit the metastasis of CTCs in vivo. MVBL combined with PTX could significantly improve the efficacy of PTX and had no obvious side effects (Fig. 4), which is clinically desirable. Both in vivo and in vitro, MVBL significantly improved

antioxidant capacity, and the associated reductions in ROS helped to inhibit tumour growth and metastasis (Fig. 5). At the animal level, MVBL enhanced the immune function of macrophages and T cells in the blood, reinforcing the body's ability to fight cancer (Fig. 5). At the selected doses, MVBL was able to significantly inhibit tumour metastasis in a mouse lung metastasis model with no additional harm to the mice themselves (Fig. 6). The safety of the four currently known and widely used component drugs of MVBL has long been accepted, and the effects of these individual drugs are known. The combination and rational application of existing drugs for more effective treatment of tumour metastasis are currently neglected. Our findings show that the MVBL drug combination is effective and causes no significant side effects. Inhibition of tumour growth and metastasis requires not only the use of chemotherapeutic drugs but also enhancement of patients' nutritional status; adjuvant drugs such as MVBL may be useful for these purposes.

Declarations

ACKNOWLEDGEMENTS

Funding

This work was supported by the National Natural Science Foundation of China (NSFC, grant numbers 81703555, 81961138017, 81773063); Natural Science Foundation of Fujian Province (grant number 2020J01859); Young and Middle-aged Teacher Education Research Project of Fujian Province(grant number JAT200412).

Data availability

The authors confirm that the data supporting the findings of this study are available within the article.

Conflict of interest

All authors declare no conflict of interest.

Authors Contributions

Y Cheng and Y Lu planned the study. S Li, Y Cheng, S Lian, Y Lu, J Wang, X Deng and S Zhai performed cell experiments and collected data. S Li, S Lian and Y Lu analyzed and interpreted data. Y Cheng and L Jia drafted manuscript and all the authors approved the draft of the submitted manuscript.

Ethics approval

The study was approved by the local ethical committee and was conducted according to the Declaration of Helsinki.

Consent to participate

All patients provided informed consent before the acquisition of their data.

Corresponding author

Correspondence to Lee Jia.

References

1. Zhou M, Wang H, Zeng X, Yin P, Zhu J, Chen W, et al. Mortality, morbidity, and risk factors in China and its provinces, 1990–2017: a systematic analysis for the Global Burden of Disease Study 2017. The Lancet. 2019;394(10204):1145-58.

2. Prasad S, Gupta SC, Tyagi AK. Reactive oxygen species (ROS) and cancer: Role of antioxidative nutraceuticals. Cancer Lett. 2017;387:95-105.

3. Crowder SW, Horton LW, Lee SH, McClain CM, Hawkins OE, Palmer AM, et al. Passage-dependent cancerous transformation of human mesenchymal stem cells under carcinogenic hypoxia. Faseb J. 2013;27(7):2788-98.

4. Ma J, Zhang Q, Chen S, Fang B, Yang Q, Chen C, et al. Mitochondrial dysfunction promotes breast cancer cell migration and invasion through HIF1alpha accumulation via increased production of reactive oxygen species. PLoS One. 2013;8(7):e69485.

5. Shimojo Y, Akimoto M, Hisanaga T, Tanaka T, Tajima Y, Honma Y, et al. Attenuation of reactive oxygen species by antioxidants suppresses hypoxia-induced epithelial-mesenchymal transition and metastasis of pancreatic cancer cells. Clinical & Experimental Metastasis. 2013;30(2):143-54.

6. Liu X, Pei C, Yan S, Liu G, Liu G, Chen W, et al. NADPH oxidase 1-dependent ROS is crucial for TLR4 signaling to promote tumor metastasis of non-small cell lung cancer. Tumor Biology. 2015;36(3):1-10.

7. Cheng CW, Kuo CY, Fan CC, Fang WC, Jiang SS, Lo YK, et al. Overexpression of Lon contributes to survival and aggressive phenotype of cancer cells through mitochondrial complex I-mediated generation of reactive oxygen species. Cell Death & Disease. 2013;4(6):e681.

8. Rayman MP. Selenium and human health : The Lancet. Lancet. 2000;356:942–3.

9. YZ F, S Y, G W. Free radicals, antioxidants, and nutrition. Nutrition. 2002;18(10):872-9.

10. X Z, WJ J, Y Z, B H, H L, TG H, et al. Enhancement of endogenous defenses against ROS by supra-nutritional level of selenium is more safe and effective than antioxidant supplementation in reducing hypertensive target organ damage. Medical Hypotheses. 2007;68(5):952-6.

11. Hagemann-Jensen M, Uhlenbrock F, Kehlet S, Andresen L, Gabel-Jensen C, Ellgaard L, et al. The selenium metabolite methylselenol regulates the expression of ligands that trigger immune activation

through the lymphocyte receptor NKG2D. Journal of Biological Chemistry. 2014;289(45):31576.

12. Roy M, Kiremidjian-Schumacher L, Wishe HI, Cohen MW. Supplementation with selenium and human immune cell functions. Biological Trace Element Research. 1994;41(1-2):115.

13. Dowd S. Long Term Dietary Supplementation of Organic Selenium Enhances Expression of Immune Related Genes in Adult Pigs. Biochemical Journal. 2012;446(3):427-35.

14. Ramadan AA, Ghoniem AA, Hassan HM, Youssef AE. Effects of beta-carotene, selenium and vitamin A on in vitro polymorphonuclear leukocytic activity in peripartal buffalo (Bubalus bubalus). Theriogenology. 2001;55(3):693-704.

15. Steinbrenner H, Speckmann B, Sies H. Toward understanding success and failures in the use of selenium for cancer prevention. Antioxidants & Redox Signaling. 2013;19(2):181-91.

16. Kaur S, Saluja M, Bansal MP. Bisphenol A induced oxidative stress and apoptosis in mice testes: Modulation by selenium. Andrologia. 2017;50(4):e12834.

17. Dong C, Sun S, Cai D, Kong G. Induction of mitochondrial-dependent apoptosis in T24 cells by a selenium (Se)-containing polysaccharide from Ginkgo biloba L. leaves. International Journal of Biological Macromolecules. 2017;101:126-30.

18. Paolini M, Antelli A, Pozzetti L, Spetlova D, Perocco P, Valgimigli L, et al. Induction of cytochrome P450 enzymes and over-generation of oxygen radicals in beta-carotene supplemented rats. Carcinogenesis. 2001;22(9):1483-95.

19. Kim YS, Lee HA, Lim JY, Kim Y, Jung CH, Yoo SH, et al. β-Carotene inhibits neuroblastoma cell invasion and metastasis in vitro and in vivo by decreasing level of hypoxia-inducible factor-1α. Journal of Nutritional Biochemistry. 2014;25(6):655-64.

20. Ibrahimhashim A, Wojtkowiak JW, De LCRM, Estrella V, Bailey KM, Cornnell HH, et al. Free Base Lysine Increases Survival and Reduces Metastasis in Prostate Cancer Model. Journal of Cancer Science & Therapy. 2011;Suppl 1(4).

21. Roomi MW, Ivanov V, Kalinovsky T, Niedzwiecki A, Rath M. In vivo antitumor effect of ascorbic acid, lysine, proline and green tea extract on human prostate cancer PC-3 xenografts in nude mice: evaluation of tumor growth and immunohistochemistry. Vivo. 2005;19(1):179.

22. Roomi MW, Ivanov V, Kalinovsky T, Niedzwiecki A, Rath M. In vitro and in vivo antitumorigenic activity of a mixture of lysine, proline, ascorbic acid, and green tea extract on human breast cancer lines MDA-MB-231 and MCF-7. Medical Oncology. 2005;22(2):129-38.

Figures

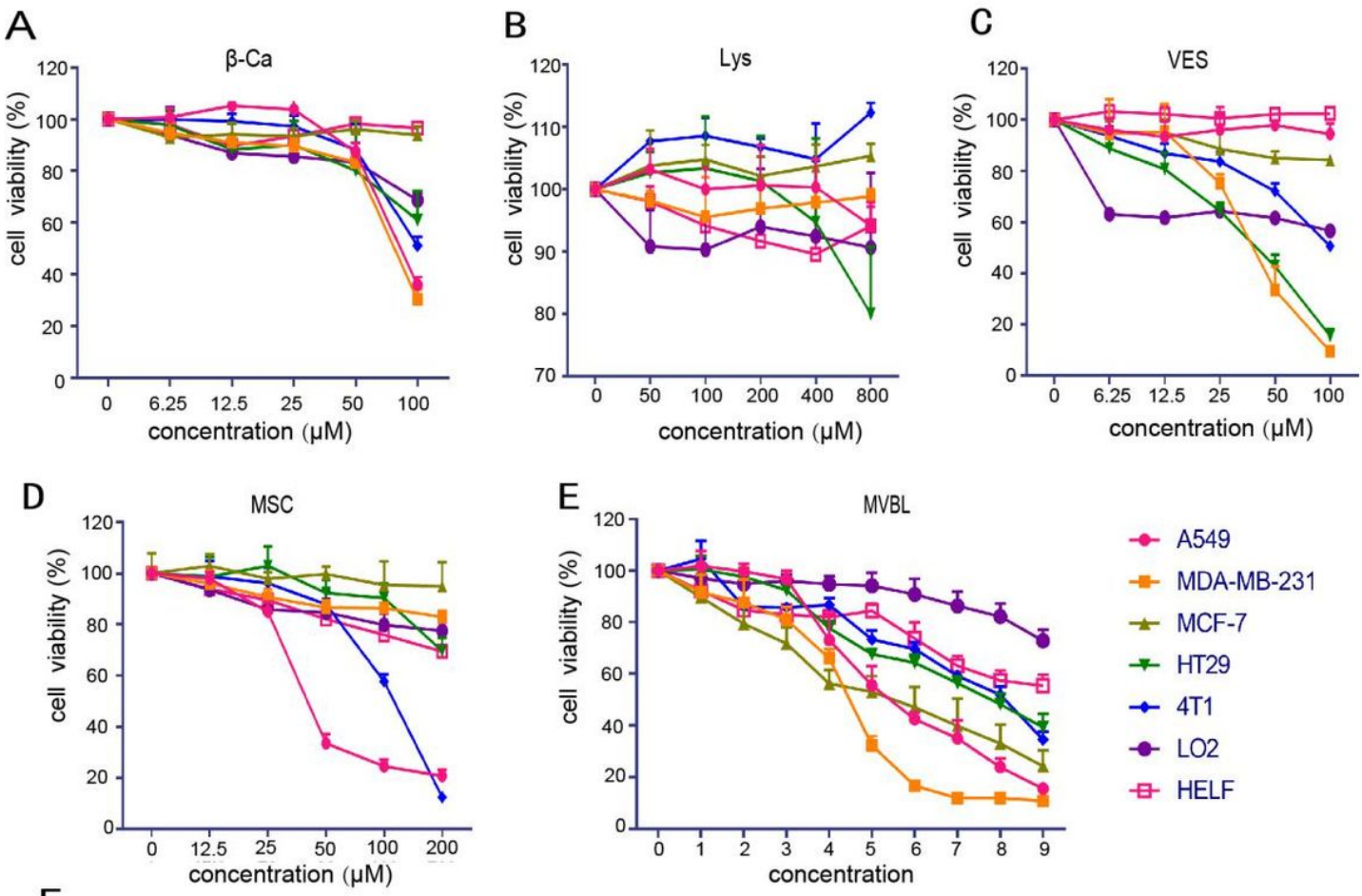

F

group / drug	C	Single drug				MVBL (μM)								
	0	2	3	4	5	1	2	3	4	5	6	7	8	9
MSC	0	25	50	100	200	2	5	10	20	30	35	40	45	50
VES	0	12.5	25	50	100	4	10	20	40	60	70	80	90	100
β-Ca	0	12.5	25	50	100	4	10	20	40	60	70	80	90	100
Lys	0	100	200	400	800	40	100	200	400	600	700	800	900	1000

Figure 1

Cytotoxicity of single drugs and MVBL toward various cell types. All cells were treated for 24 h. (A) Effect of β-Ca on the viability of MCF-7/HT29/MDA-MB-231/A549/4T1/LO2/HELF cells. (B) Effects of Lys on the viability of cells. (C) Effects of VES on the viability of cells. (D) Effects of MSC on the viability of cells. (E) Effects of MVBL on the viability of cells. MVBL was more toxic to tumour cells than to normal cells. (F) Single drug and MVBL concentrations. The bars represent the means ± SDs (n = 5).

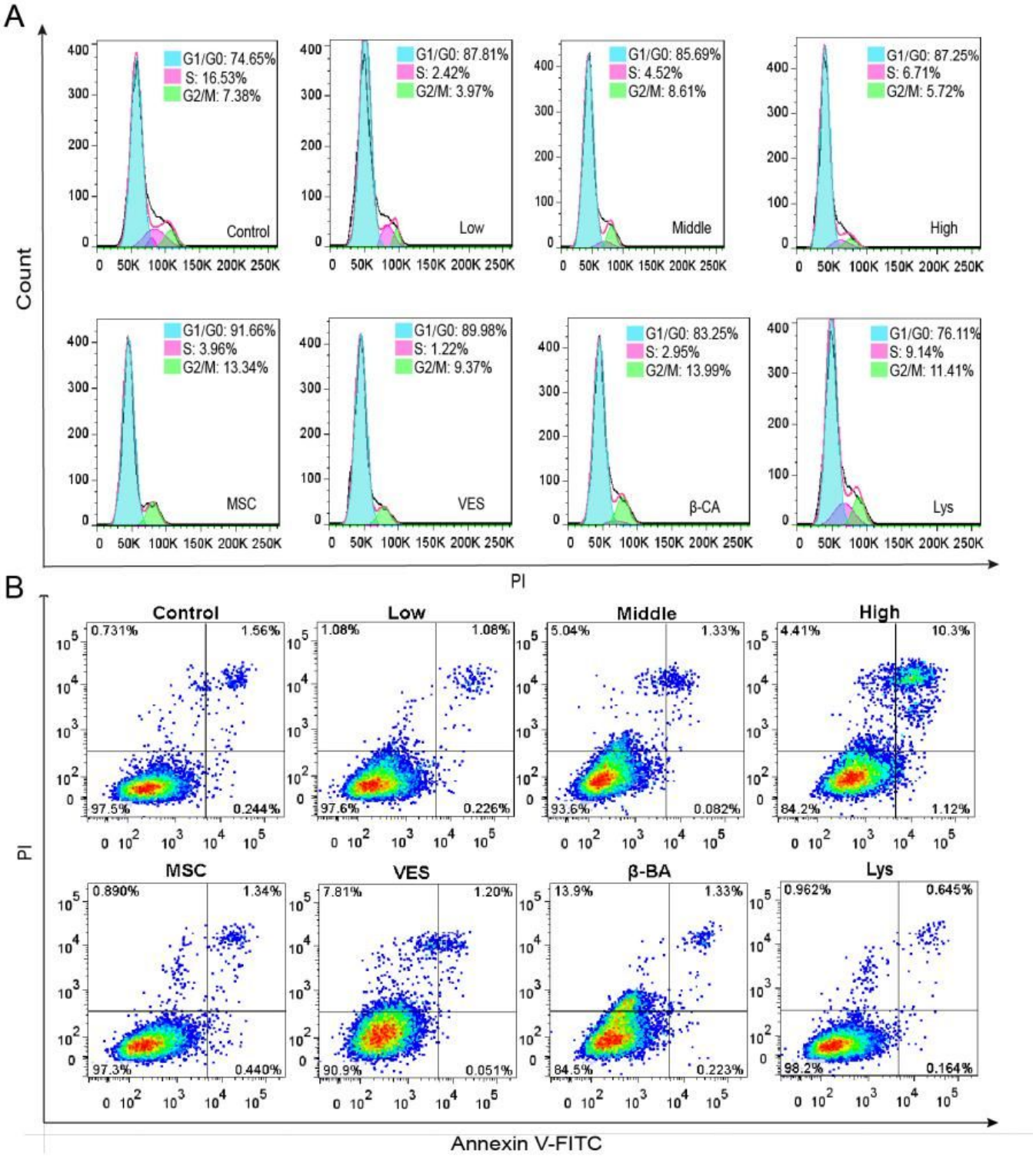

Figure 2

Effects of MVBL and single drugs on the cell cycle and apoptosis in A549 cells. The cells were incubated with MVBL and the single drugs for 24 h. (A) There was no significant change in the cell cycle, as detected by flow cytometry. (B) Apoptosis increased with increasing MVBL concentration.

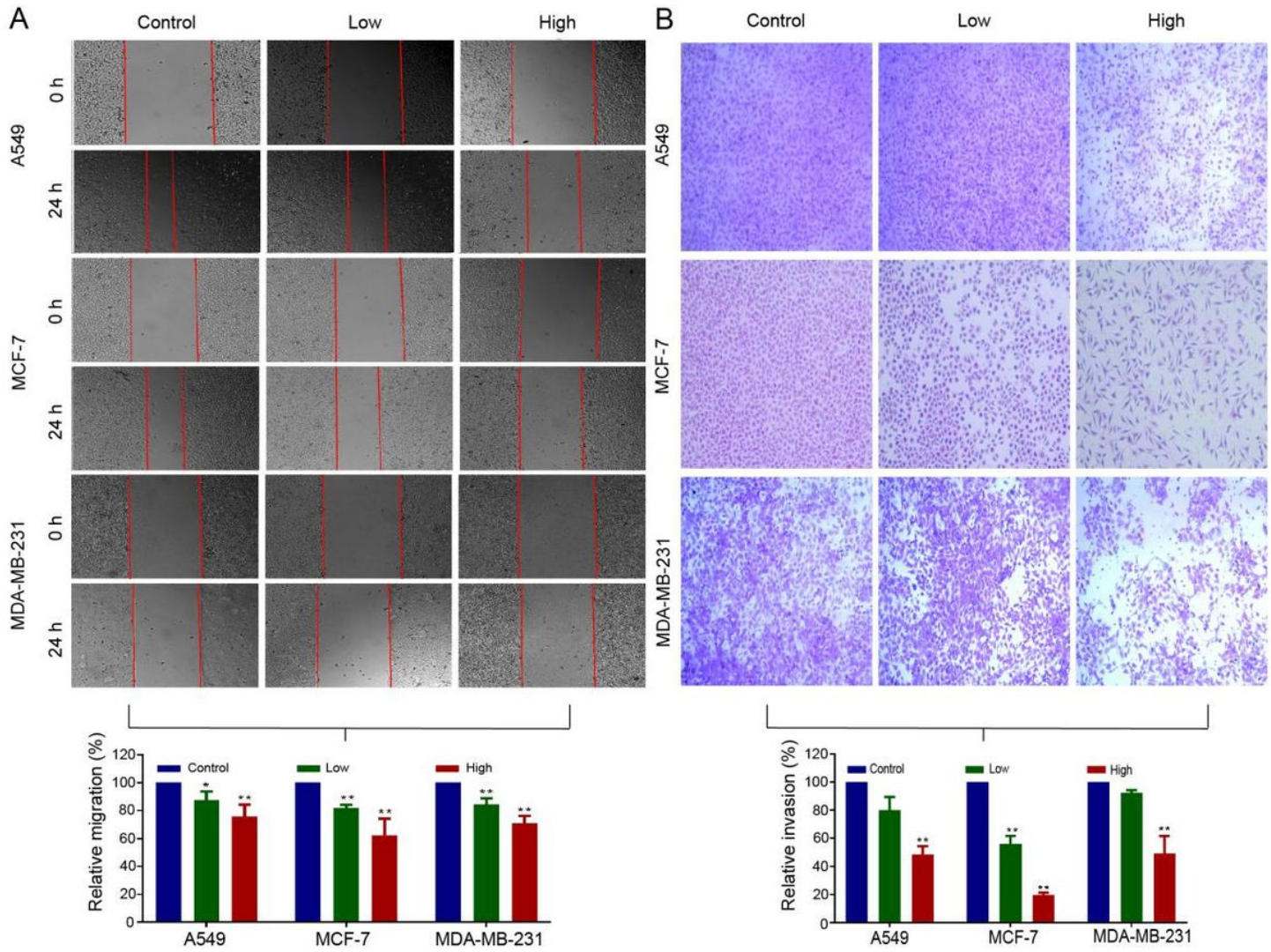

Figure 3

MVBL inhibited A549/MCF-7/MDA-MB-231 cell migration and invasion. After 24 h of treatment at the selected low and high concentrations, the effect was found to increase with concentration. (A) The cell migration distance of the treated cells was shorter than that of the control cells. (B) Numbers of cells that passed through the membrane after treatment with different drug concentrations. The bars represent the means ± SDs (n = 3); * indicates $P < 0.05$; **, $P < 0.01$.

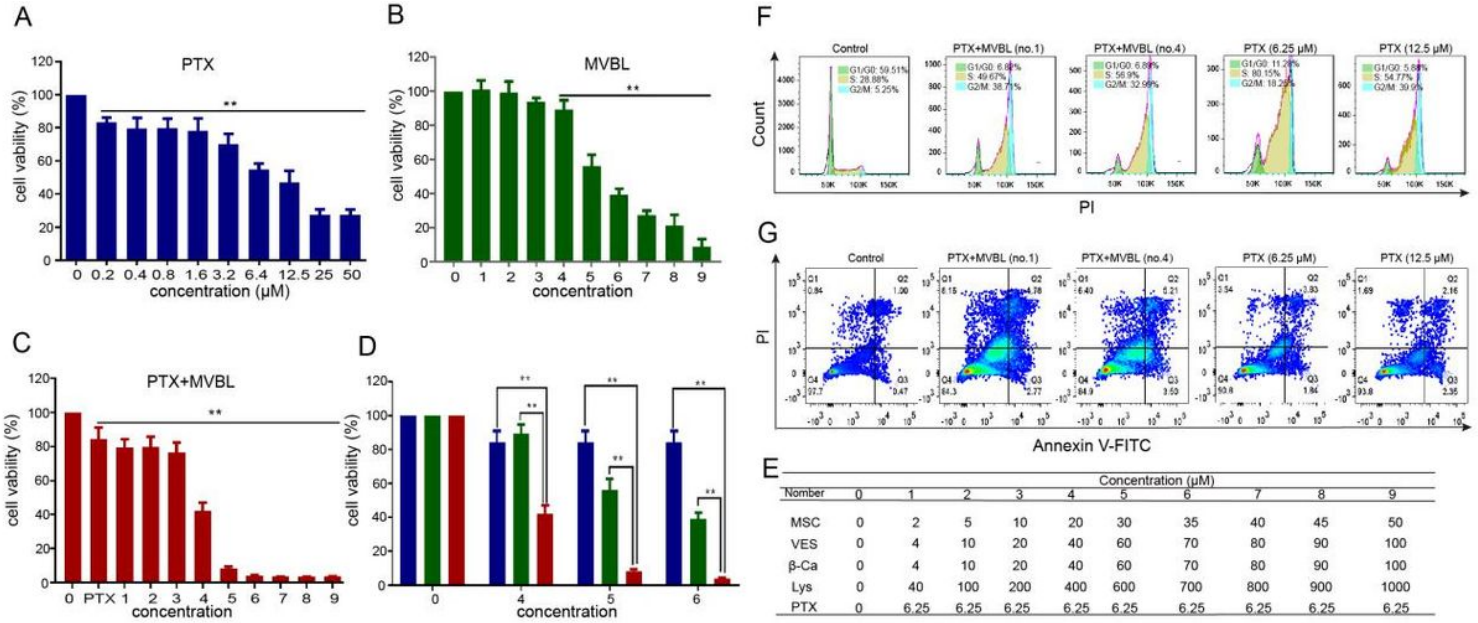

Figure 4

Effects of MVBL combined with PTX on MDA-MB-231 cells. The cells were incubated with the drugs for 24 h. (A) The cells were treated with PTX. (B) The cells were treated with MVBL. (C) PTX at 6.25 μM was combined with different concentrations of MVBL (nos. 1-9). (D) PTX (6.25 μM) combined with MVBL (no. 4/5/6) was very cytotoxic. (E) Concentrations of PTX and MVBL. (F) Cell cycle distributions (control, PTX (6.25 μM)+MVBL (no. 1), PTX (6.25 μM)+MVBL (no. 4), PTX (6.25 μM), and PTX (12.5 μM)). (G) Apoptosis (control, PTX (6.25 μM)+MVBL (no. 1), PTX (6.25 μM)+MVBL (no. 4), PTX (6.25 μM), and PTX (12.5 μM)). The bars represent the means ± SDs (n = 5); * indicates $P < 0.05$; **, $P < 0.01$.

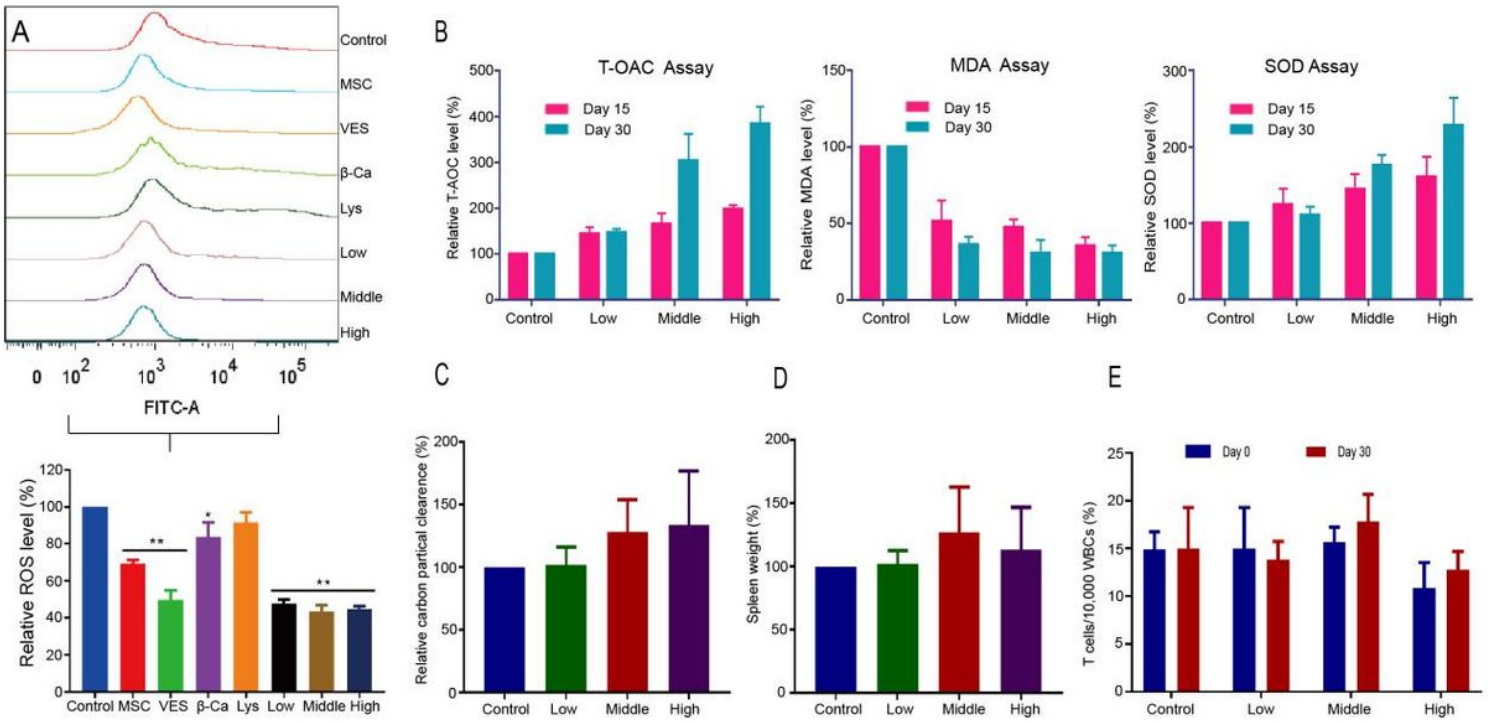

Figure 5

Results of oxidative and immune function studies. (A) Effects of MVBL and single drugs on ROS levels in MCF-7 cells after 24 h. (B) Changes in T-AOC/MDA/SOD levels on days 0/15/30 of dosing in vivo. Antioxidant ability in mice was greatly enhanced by treatment. (C) Carbon clearance. (D) Spleen weight. (E) Number of T cells per 10,000 white blood cells (WBCs) as detected by flow cytometry on days 0 and 30. The bars represent the means ± SDs (n =10).

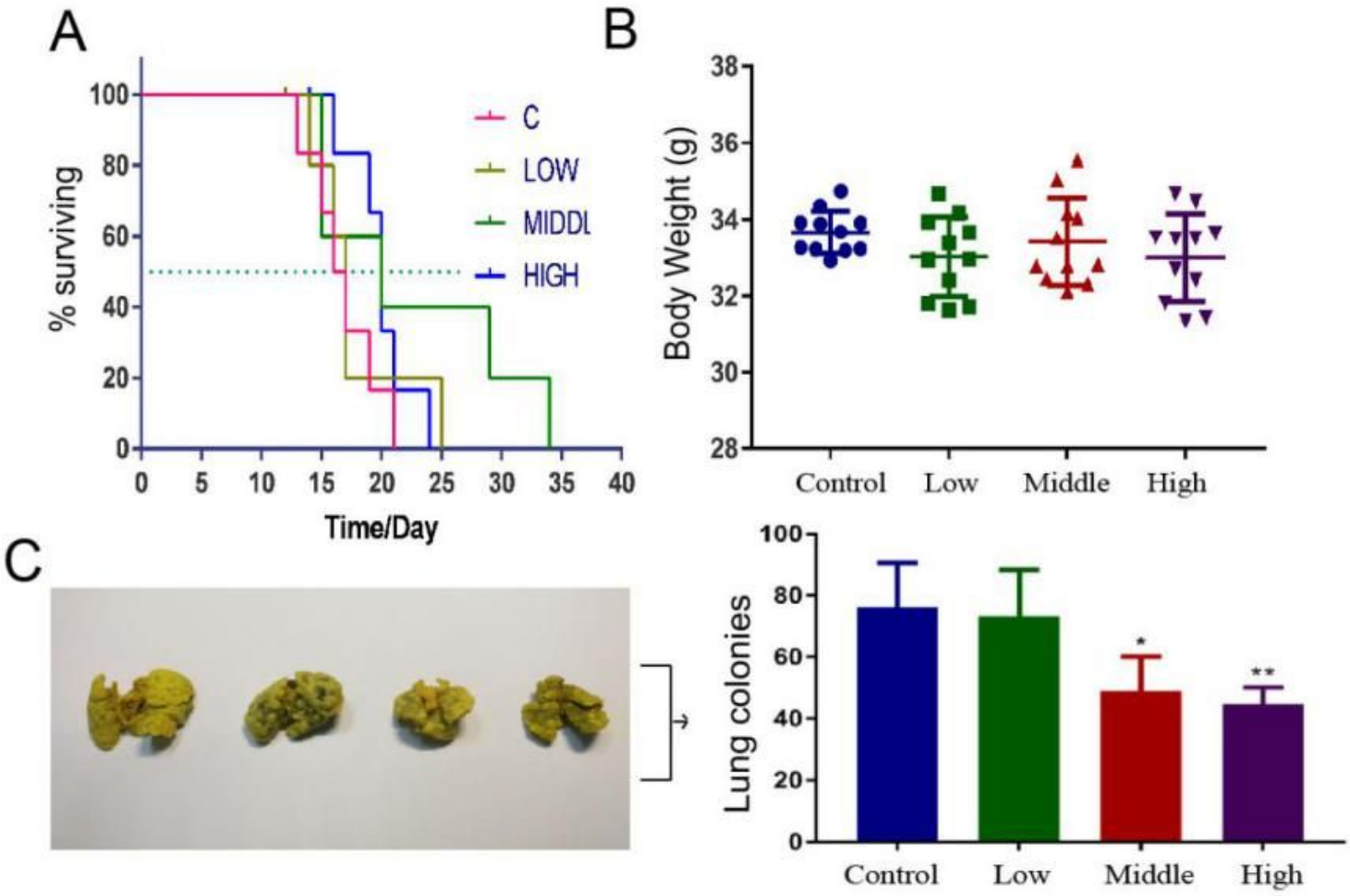

Figure 6

Inhibition of tumour metastasis by MVBL in vivo. (A) Average survival times of mice in the control group (16.5 days), the low-dose group (17 days), the medium-dose group (21 days), and the high-dose group (20 days). (B) Mouse weight. (C) Number of lung metastases. The bars represent the means ± SDs (n = 6).

Supplementary Files

This is a list of supplementary files associated with this preprint. Click to download.

- SupplementInformation.docx